/N-36
219438
21P

NASA TECHNICAL MEMORANDUM (NASA) TT-20077

LASER ANEMOMETRY TECHNIQUES FOR HOT FLOWS

P. Kugler, G. Langer

GERMANY, FEDERAL REPUBLIC OF, IN: Analysis of propellants and explosives: Chemical and physical methods; Proceedings of the 17th Int. Annual Conf., Karlsruhe, W. Germany, June 25-27, 1986 (A87-27201 10-28), Pfinztal, West Germany, Fraunhofer-Institut fuer Treib- und Explosivstoffe, 1986, p. 29-1 to 29-14.

NATIONAL AERONAUTICS AND SPACE ADMINISTRATION

WASHINGTON, D.C. 20546

Summary

Anemometry is used for the analysis of velocity and turbulence in flows. The most widely used types, difference Doppler anemometry and Laser Transit Anemometry, are presented. Correlation methods are used successfully for signal processing in hot supersonic free jets. These are explained and results presented for a hot supersonic free jet.

For signal processing in instationary flows, the suitability of an opto-acoustic demodulation method is tested and the results discussed. A measuring concept for instationary flows is proposed.

Introduction

To determine the local velocity distribution and its time fluctuations, laser-optic methods have proven suitable in flow engineering. Stationary single- and multi-phase flows can be determined in a broad temperature range with high local resolution. The measuring range covers velocities from 10^{-6} to several 10^3 m/s. These measuring methods are called Laser Anemometry. Their operation is based on determining and processing the chronology of scattered light from microparticles in the flow in a measured volume defined by laser light. Most widely used are Difference-Doppler Anemometry and Laser-Transit Anemometry. Both methods are described and the techniques of signal processing best suited for analysis of fast, hot flows, are presented. Results of measurements on a hot, supersonic free jet are presented.

A device for opto-electronic demodulation of Laser-Doppler signals [1] was constructed and its suitability for determining instationary flows was investigated. The results are also provided.

1. Difference-Doppler Anemometry

Doppler anemometry and its most common use as Difference-Doppler Anemometry (DDA), are described in the literature. An extensive presentation is found in [2, 3, 4, and 5]. The principle of DDA is shown in fig. 1. Two coherent partial beams emitted from a laser intersect at an angle 'alpha' in the measured volume. A particle with velocity v crosses the volume at an angle 'beta' relative to the middle axis of the two beams. This scatters the light which undergoes a Doppler shift at an angle 'theta-2' for an observer. This Doppler shift is given by the wavelength 'lambda' of the incident beam, the angle 'theta-1' and the angle of observation 'theta-2'. At the same time, a Doppler shift occurs compared to the second beam, as a function of 'theta-1'', 'theta-2', $|\overline{v}|$ and 'beta'. The difference frequency f_D of the two Doppler shifts becomes:

$$f_D = \frac{|\overline{v}|}{\lambda} \, 2 \cos \beta \sin (\alpha/2) \qquad (1)$$

and is independent of the point of observation. The interference-strip model provides an illustration. The two beams form an interference pattern in their intersection volume, whose strip interval s (fig. 2) is defined as:

$$s = \frac{\lambda}{2 \sin (\alpha/2)} \qquad (2)$$

A particle of velocity $\vec{v}$ moving at an angle 'beta' through the strip plane, scatters a light signal which is modulated by the intensity distribution in the laser beam and by equation (2). Possible signal forms are shown in fig. 3 (from [5]), and fig. 3a shows the signal of a particle flying through the middle of the interference region and whose diameter is smaller than the interference strip spacing.

Figure 3b shows a less well modulated signal. Here, either the particle is large compared to the interference strip spacing, or the partial beams forming the measured volume are of unequal intensity. The signal of a particle which crosses the two partial beams outside the intersection midpoint, is shown in fig. 3c.

The observed Doppler frequency is a direct measure for the velocity component $\vec{v}$ perpendicular to the interference strip plane, but is independent of the sign of the velocity vector. Additional information on the velocity direction is obtained e.g., by frequency-shifting the two beams by means of one or two Bragg cells, and at a difference frequency $\Delta \nu$, the interference strip pattern moves at velocity:

$$v_f = \frac{2 \Delta \nu \lambda}{2 \sin (\alpha/2)} \qquad (3)$$

in the direction of the higher-frequency beam and the Doppler frequency increases or decreases according to its direction.

1.1 Signal Processing for Stationary Flows

The result of the measurement of velocity of a scattering center when crossing the measured volume is a so-called Doppler burst, whose intensity I(t) at the output of the photodetector at constant velocity v is described by:

$$I(t) = I_0 [1 + \cos(2\pi f_D)] (\exp - (\frac{v (t - t_0)}{D})^2) \tag{4}$$

I_O is a function of the scattered light conditions (particle size, velocity, intensity of the source, scattering characteristics), f_D = Doppler frequency and D = diameter of the measured volume whose middle is crossed at $t = t_O$. The goal of signal processing is the determination and storage of the Doppler frequency of as many Doppler signals of individual particles and their statistical behavior. For stationary flows, counter methods, trackers, spectrum analyzers and correlation techniques are used.

1.1.1 Counter Method

Frequncy measurement is performed by time counting of a filtered and selected Doppler burst. This must be clearly distinguished from the noise. The method is suitable for measurements in fluids and clean gas flows. Our own work on a hot free jet has shown that the signal quality is not sufficient for counter processing, given the microparticles used for doping the beam.

1.1.2 Tracker Method

The Doppler frequency to be measured, is compared with the frequency of a voltage-controlled oscillator (VCO) and from the phase difference between the two signals, the burst frequency is deduced via a control circuit of the VCO. The measure for burst frequency is the control voltage of the VCO. The method requires a high signal sequence, i.e. particle density, and not too much frequency fluctuation. The method is not suitable for instationary flows, fast velocity changes and qualitatively fast Doppler signals.

1.1.3 Spectrum Analyzer

The Doppler signal is compared with a continuously wobbled frequency. In case of agreement, the control voltage of the wobbler is stored as a measured value. Due to the method, only a few bursts are demodulated, so its use with instationary flows is not possible.

The method is suitable for obtaining an overveiw of the statistics of the Doppler signals in stationary flows. It is an advantage that no arbitrary signal selection is made.

1.1.4 Correlation Method

This method uses single photon counting for detection of scattered light and the burst information is obtained as a normed pulse sequence whose probability density is given with respect to equation 4 (fig. 4). Processing occurs via a digital correlator which forms the autocorrelation function of the input signal from the pulse input sequence. A detailed description of the principle is found in [4]. Its operation is shown in fig. 5. The pulse density signal is multiplied with a clocked shift register with its own prehistory and summed in the memories allocated to each element of the shift register. The saved values of the memory register form the average values of the autocorrelation function

(AKF) computed about the particular shift clock. The qualitative profile of the AKF is shown in fig. 5 as a dashed line. The average value of burst frequency is reflected in the frequency information of the AKF; the frequency fluctuation (corresponding to turbulence) shows up in the decay of the AKF.

For the evaluation, further processing of the stored AKF (using computer programs) is necessary, and this requires a suitable modelling for signal statistics.

The advantage of the correlation method is that all information arriving in the measurement interval can be used to form the AKF and even noisy signals can have their information extracted by stochastic computations. An analysis of instationary flow phenomena is not possible, since the AKF contains the summed information over the entire measurement time. The processable Doppler frequencies are limited by the shift clock time.

Our own work on a 50 ns correlation has shown that velocity measurements can be taken with good average value quality, low turbulence and relatively imprecise turbulence degree, in hot supersonic free jets up to the range of 1500 m/s [6]. New correlators with shift clock times down to 10 ns are available for such measurements.

2. Laser Transit Anemometry

A method for measuring the transit time behavior of scattered particles in flows was suggested in 1968 by Thompson [7]. By using a cylinder lens, a divided laser beam was imaged in the measured volume so that two narrow light strips are formed perpendicular to the flow direction. A scattered particle passing the two beams in the flow direction, emits light in each of the two beams, which is detected by a photomultiplier. It causes two voltage peaks at the multiplier output, whose time sequence corresponds to the transit time of the particle. This method was refined by Schodl [8] for measurements on turbine blades. A prerequisite for transit anemometry is that the primary flow direction be known, or determinable by rotating the measuring plane.

Time/amplitude converters with outlet-connected multi-channel analyzers or correlation methods are used for processing.

2.1 Transit Anemometry with Multi-Channel Analyzer

The two partial beams are observed through one photomultipler each. Upon passage of a particle which is crossing the first partial beam in the flow direction, a time/amplitude converter is started and then stopped when the particle crosses the second beam. The pertinent amplitude value is digitized and stored in a multi-channel analyzer (VKA). It is also possible to use a time/digital converter which starts a very fast counter with the first pulse and which is stopped with the second. The average transit time corresponds to the position of the maximum peak in the VKA, the fluctuation width is represented by the width of the peak. A disadvantage of this method is the processing-related dead times. Measurement of instationary flows is not possible, due to the processing principle.

2.2 Transit Anemometry with Cross Correlation

The two single beams are observed through one photomultiplier each. Processing is similar to fig. 5, but the signal from photomultiplier 1 is allocated to the shift register; the signal from photomultipler 2 is allocated to the "and"-links. The cross correlation function of the two detectors is formed in the register memories. It forms a peak whose location corresponds approximately to the average transit time for low turbulence. Position and shape of this peak per Durrani and Greated [9, 3] become:

$$R_c(sT) = \alpha^2 T^2 (\lambda_1 + B_0 C_0)(\lambda_2 + B_0 C_0) + + \frac{B_1 C_0 d_0}{(2\pi\sigma^2 (sT)^4)^{1/2}} \exp\left\{- \frac{1}{2\sigma^2} (U_0 - d_0/sT)^2\right\} \tag{5}$$

'alpha' = quantum efficiency of the photo detector, U_o = average flow velocity, $\bar{\sigma}^2$ = average quadratic turbulence, T = shift clock time, 'lambda-1' and 'lambda-2' describe the background noise, B_o, B_1 and C_o characterize the distribution of scattered particles in the flow. For practical measurements, this function can be reduced to the following expressing [10], when the test parameters are held constant:

$$R_c(sT) = C_1 + \frac{C_2}{\sigma s^2 T^2} \exp\left\{- \frac{1}{2\sigma^2} (U_0 - d_0/sT)^2\right\} \tag{6}$$

and after determining the background portion C_1, the parameters C_2, 'sigma' and U_o can be determined.

No information is lost due to dead times in the correlation methods, and yet useful KKF can still be obtained when the useful signals lie below the noise.

3. Results of Laser-Transit Method on Hot Free Jets

Laser-transit measurements were taken on a small, liquid rocket motor. The mass throughput of the water-cooled motor was 70 Nm^3 O_2 and 30 l C_2H_5OH per hour; chamber pressure 4.8 bar, exhaust temperature 2200 - 2500 K. The computed gas velocity was ca. 1400 m/s.

An argon-ion laser of 1500 mW output power at 488 nm, and an ITT FW 130 and an EMI RR 127 photomultiplier were used. For signal processing, a Malvern K 7023 correlator with a shift clock of 50 ns was used.

The flow was first optimized until no information carriers (e.g. soot, droplets) were observed in the exhaust jet. Then the TiO_2 particles of average 0.3 u diameter were added to the flow. The measured KKF shows very good S/N ratio; fig. 6 shows a typical measurement. To determine the average velocity and the degree of turbulence, is was not possible to approximate the measured curves per a modelling law per equation (6). In nearly all the several hundred measured curves, two maxima peaks were found in the KKF, which indicate the presence of two average velocities. So equation (7) was expanded to:

$$R_C(sT) = C_1 + \frac{C_2}{\sigma s^2 T^2} \exp\{-\frac{1}{2\sigma^2}(U_1 - d_0/sT)^2\} + \frac{C_3}{\sigma s^2 T^2} \exp\{-\frac{1}{2\sigma^2}(U_2 - d_0/sT)^2\} \tag{7}$$

with the two average velocities U_1 and U_2. The 6 unknown parameters were determined with a least-squares fit program. From the computed x^2-errors, the error of the individual parameters was determined by using an error analysis. The statistical error of the primary maxima of the KKF were between 0.3 and 0.75%, for the secondary maxima, between 1.17 and 1.54%. The error for the degree of turbulence was between 4.1 and 5.4%. The error analysis justifies the modelling assumptions. Velocity distribution and degree of turbulence over 3 nozzle diameters along the middle axis are shown in fig. 7. The error intervals are also shown. The velocity profile shows that the added TiO_2 particles are able to follow the flow accurately. The duration of measurement per point was several seconds on average. But a few milliseconds are sufficient for a satisfactory peak detection.

4. Evaluation of the Method

The work has shown that it is possible to measure stationary, hot supersonic free jets. Transit anemometry in connection with digital cross correlation proved to be best suited for this. But the DDA can be used with digital auto correlation, provided fast correlators are available. Determination of instationary flows is not possible with any of the listed signal processing methods.

But actually the instationary flows are of interest for the investigation of the behavior of liquid, tube-weapon propellents and transient combustion processes. A signal processing method for opto-acoustic Fourier transformation was proposed by Schnettler [1] and was investigated for its utility.

5. Opto-acoustic Demodulation of Laser-Doppler Signals

The nucleus of the demodulator is a Bragg cell which operates as an opto-acoustic Fourier transformer. A piezo-quartz crystal converts the HF electric input signal into acoustic waves which run through an optically permeable crystal. They cause a local refractive index variation in the crystal, which acts as an optic grid for the passing laser beam. Upon incidence at less than the Bragg angle, the maximum intensity of the beam is subject to 1st order diffraction. A frequency change of the input signal causes a shift in lattice spacing and thus a change in diffraction angle.

5.1 Test Set-up for Opto-acoustic Demodulation

To investigate the capability of such a device, the arrangement per fig. 8 was set up. The used Bragg cell has a middle frequency of 80 MHz. In order to check the largest possible frequency range, the burst signal of frequency f_D to be investigated, was mixed in an amplitude modulator with a carrier frequency of f_o = 80 MHz, and the output signals f_o, f_o+f_D and f_o-f_D are obtained. This frequency mixture was fed via a power amplifier to the piezo-elements at the Bragg cell having input power from a 5 mV HeNe laser. The Doppler burst was synthesized by using another electronic assembly. The base frequency f_D and the number of wave cycles n contained in the burst, were variable. The goal of the investigation was to obtain information about the attainable frequency range and the minimum necessary number of wave cycles. The deflection of the laser beam was observed visually on a screen. A detailed illustration is found in [11].

5.2 Test Results for Opto-acoustic Demodulation

The position of the 1st order maximum relative to the 0-order was observed at a distance of ca. 1 m from the Bragg cell. The results are summarized in fig. 9. The right side band of the deflected beam is shown. Figure 9a shows the range of the arrangement at a carrier frequency f_o of 80 MHz and a Doppler frequency of 50 MHz at 20 cycles. The obtained mixed frequencies of 80, 30 and 130 MHz can still be processed. At a Doppler frequency of 5 MHz at 20 cycles, the deflected beams easily flow into each other (fig. 9b). But for greater distance from the screen, resolutions of 1 MHz are still attained. The behavior as a function of the number of Doppler cycles is shown in fig. 9c (f_D = 50 MHz, f_o = 80 MHz). At 20 Doppler cycles, one obtains a sharp-edge diffraction of 1st order for 130 MHz, for 3 cycles it is easily blurred and at only one cycle, the deflection is still discernable. This means that even very poor, real Doppler signals still cause a unique allocation of Doppler frequency and diffraction behavior.

The intensity of the 1st order diffracted laser portion is dependent on the amplitude of the Doppler burst.

5.3 Measurement Concept with Opto-acoustic Demodulation

This type of demodulator can be constructed as follows: To increase the operating range, the carrier can be reduced to ca. 50 MHz. The modulation mixture from f_o, f_o+f_D and f_o-f_D can be restricted with filters, or better, by a one-side band modulator, to f_o+f_D. The Doppler burst must be elevated by a suitable amplifier to a constant amplitude value. Detection of the deflection can be attained with an arrangement of wedge filter and photodiode [12]. The frequency information is available as analog voltage and can be determined by conventional means. Figure 10 shows a corresponding measurement design.

6. Conclusions

The completed investigations have shown that the measurement of stationary flows is possible, even in the boundary case of hot, supersonic free jets, by using anemometry and correlation techniques. The opto-acoustic demodulation method appears to be a useful method for analysis of instationary flows.

7. References

[1] Schnettler, A.: Optoelectronic Demodulation of Laser-Doppler Signals. Dissertation RWTH Aachen, 1980.

[2] Durst, F., Melling, A., Whitelaw, J.J.: Principles and Practice of Laser-Doppler-Anemometry. Academic Press, London, 1976.

[3] Durrani, T.S., Greated, C.A.: Laser Systems in Flow Measurement. Plenum Press, New York, 1977.

[4] Cummins, H.Z., Pike, E.R.: Photon Correlation Spectroscopy and Velocimetry. Proc. of NATO Advanced Study Institute, Capri 1976, Plenum Press, New York and London, 1977.

[5] Drain, L.E.: The Laser Doppler Technique. John Wiley & Sons, Cichester - New York - Brisbane - Toronto, 1980.

[6] Kugler, H.P.: Laser Anemometry Investigations to Determine the Velocity and Density Distribution of Particles in a Rocket Exhaust Jet. ICT Report 13/1977.

[7] Thompson, D.H.: A Tracer-Particle Fluid Velocity Meter Incorporating a Laser. Journal of Physics E. 1 (1968), p. 929.

[8] Schodl, R.: A Laser-Dual Beam Method for Flow Measurements in Turbomachines. ASME Paper 74-6T-157 (1974).

[9] Durrani, T.S., Greated, C.A.: Spectral Analysis and Cross-Correlation Techniques for Photon Counting Measurements on Fluid Flows. Applied Optics, 14, 778 (1975).

[10] Kugler, H.P.: Recent Results in Rocket Exhaust Anemometry. Physica Scripta, Vol. 19 pp. 447-452, 1979.

[11] Hauck, A., Kugler, H.P., Langer, G.: Opto-electronic Demodulation of Laser-Doppler Signals. ICT Technical Report 8/85.

[12] Eisenreich, N., Kugler, H.P., Liehmann, W.: Simple Optical Method for Analog Path Measurement of Dynamic Processes. ICT Report 4/81.

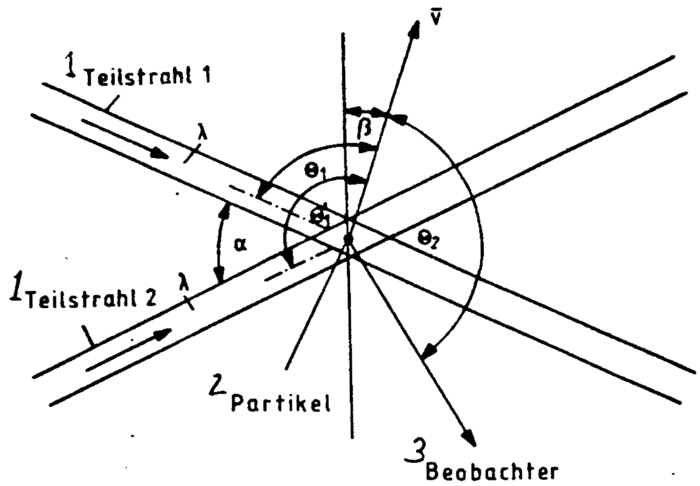

Fig. 1: Principle of the Difference Doppler Anemometer

Key: 1-partial beam 2-particle 3-observer

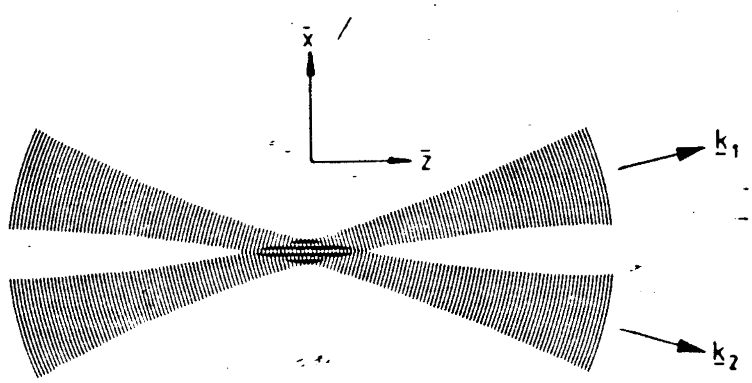

Fig. 2: Interference Strip Model

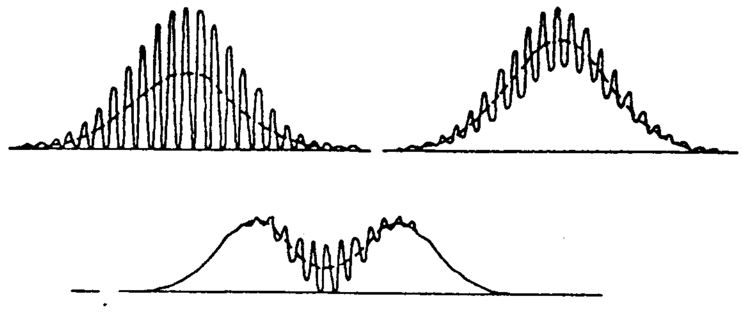

Fig. 3: Typical Signal Shapes (from [5]).

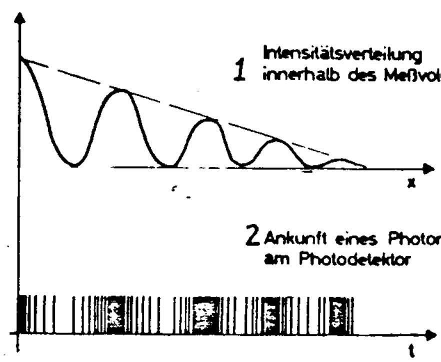

Fig. 4: Pulse Density Signal

Key: 1-intensity distribution within the volume 2-arrival of a photon at the photodetector

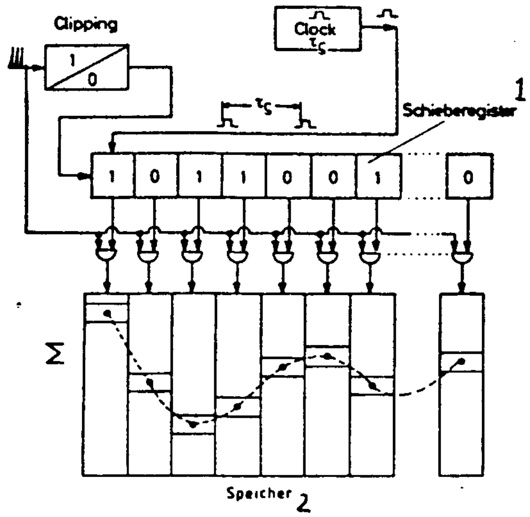

Fig. 5: Operation of the Digital Correlator

Key: 1-shift register 2-memory

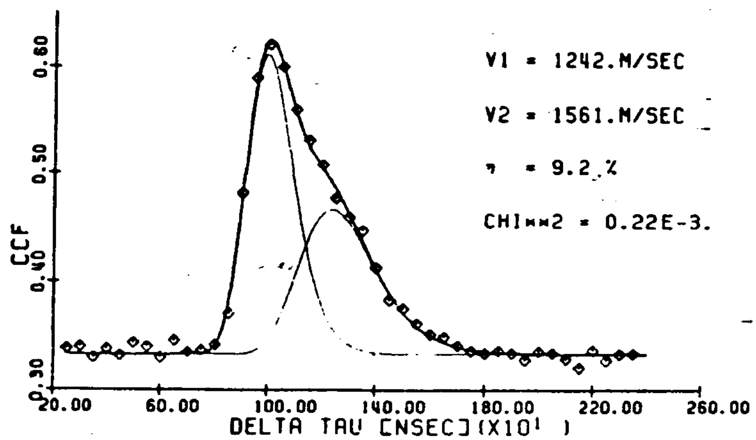

Fig. 6: Measured Cross-Correlation Function

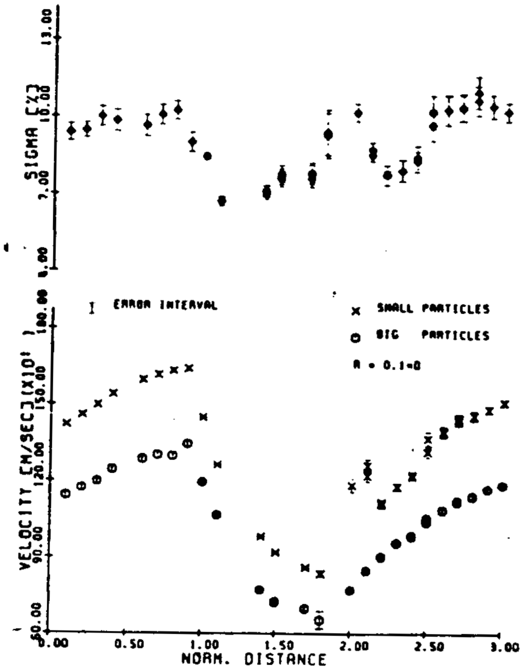

Fig. 7: Velocity and Turbulence in the Middle Axis of the Measured Rocket Free Jet

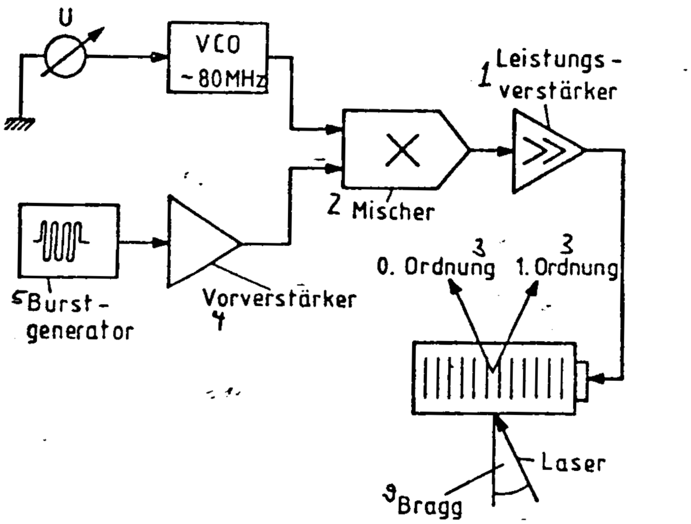

Fig. 8: Block Diagram, opto-acoustic Demodulator

Key: 1-power amplifier 2-mixer 3-order 4-preamplifier 5-burst generator

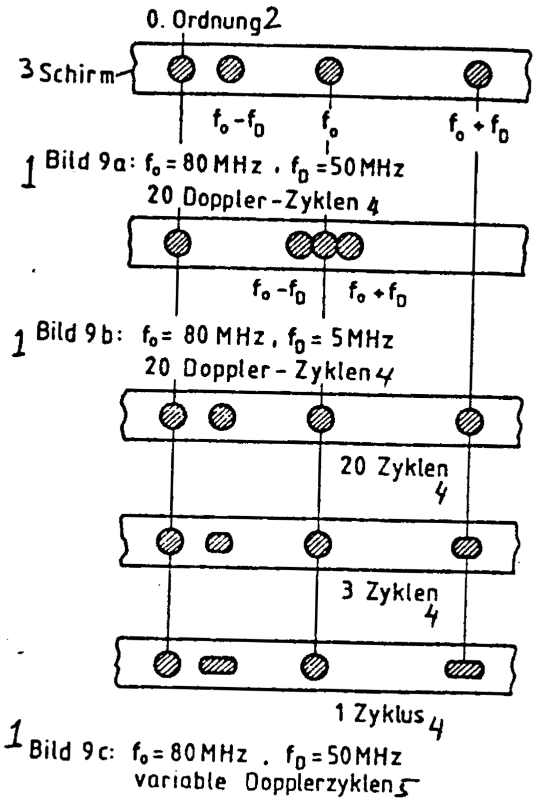

Fig. 9: Diffraction Patterns

Key: 1-figure 2-order 3-shield 4-cycles 5-variable Doppler cycles

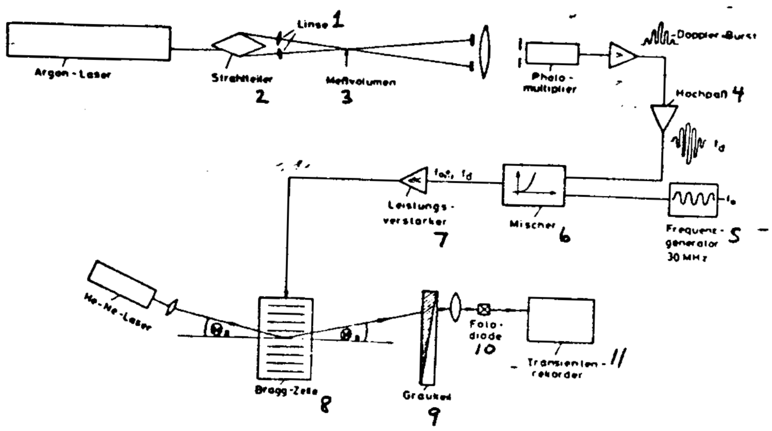

Fig. 10: Measurement Concept for Instationary Flows

Key: 1-lens 2-beam splitter 3-measured volume 4-high pass 5-frequency generator 6-mixer 7-power amplifier 8-Bragg cell 9-wedge filter 10-photo diode 11-transient recorder

STANDARD TITLE PAGE

1. Report No. TT 20077	2. Government Accession No.	3. Recipient's Catalog No.
4. Title and Subtitle Laser Anemometry for Hot Flows		5. Report Date July 87 6. Performing Organization Code
7. Author(s) P. Kugler, G. Langer		8. Performing Organization Report No. 10. Work Unit No.
9. Performing Organization Name and Address Leo Kanner Assoc. Redwood City, CA 94063		11. Contract or Grant No. 13. Type of Report and Period Covered Translation
12. Sponsoring Agency Name and Address NASA Washington, D.C.		14. Sponsoring Agency Code

15. Supplementary Notes

16. Abstract

The fundamental principles, instrumentation, and practical operation of LDA and laser-transit-anemometry systems for measuring velocity profiles and the degree of turbulence in high-temperature flows are reviewed and illustrated with diagrams, drawings and graphs of typical data. Consideration is given to counter, tracker, spectrum-analyzer and correlation methods of LDA signal processing.

17. Key Words [Selected by Author(s)]	18. Distribution Statement A87-27213 (ORIGINAL)

19. Security Classif. (of this report) Unclassified	20. Security Classif. (of this page) Unclassified	21. No. of pages	22.